

# The extraordinary Hall effect in coherent epitaxial $\tau$ (Mn,Ni)Al thin films on GaAs

T. Sands, J. De Boeck,<sup>a)</sup> J. P. Harbison, A. Scherer, H. L. Gilchrist, T. L. Cheeks, P. F. Miceli, R. Ramesh, and V. G. Keramidas  
Bellcore, 331 Newman Springs Road, Red Bank, New Jersey 07701-7040

Ultrathin coherent epitaxial films of ferromagnetic  $\tau(\text{Mn,Ni})_{0.60}\text{Al}_{0.40}$  have been grown by molecular beam epitaxy on GaAs substrates. X-ray scattering and cross-sectional transmission electron microscopy measurements confirm that the  $c$  axis of the tetragonal  $\tau$  unit cell is aligned normal to the (001) GaAs substrate. Measurements of the extraordinary Hall effect (EHE) show that the films are perpendicularly magnetized, exhibiting EHE resistivities saturating in the range of 3.3–7.1  $\mu\Omega\text{-cm}$  at room temperature. These values of EHE resistivity correspond to signals as large as +7 and –7 mV for the two magnetic states of the film with a measurement current of 1 mA. Switching between the two magnetic states is found to occur at distinct field values that depend on the previously applied maximum field. These observations suggest that the films are magnetically uniform. As such,  $\tau(\text{Mn,Ni})\text{Al}$  films may be an excellent medium for high-density storage of binary information.

## I. INTRODUCTION

High-density nonvolatile semiconductor-based memories have the potential to replace rigid magnetic disk storage in applications that demand high performance and reliability. Conventional rewritable semiconductor memory technologies, i.e., static and dynamic random access memories (SRAM and DRAM), however, must be backed up by batteries to attain nonvolatility. Programmable read-only memories such as flash achieve nonvolatility through stored charge at the cost of limited erase/write speed and endurance. Still a third category of nonvolatile memories, represented by ferroelectric and magnetoresistive RAMs, owe their nonvolatility to the inherent hysteretic properties of the materials. Although this latter approach is the most elegant, the *potential* for achieving ferroelectric or magnetoresistive RAM chips at high enough densities (e.g., 64 Mbits) to seriously challenge magnetic disk storage has not been demonstrated.

We have recently begun to explore an alternative magnetotransport approach to fabricating nonvolatile memory elements on a semiconductor substrate. The approach is based on the “extraordinary” or “anomalous” Hall effect, a transverse voltage generated in response to the asymmetric scattering of electrons from magnetic species in a ferromagnetic material.<sup>1</sup> We have previously shown that the metastable magnetic phase  $\tau\text{MnAl}$  can be grown by molecular beam epitaxy (MBE) on {001}AlAs/GaAs with an orientation relationship that aligns the easy magnetic axis of  $\tau\text{MnAl}$  (the  $c$  axis of the tetragonal unit cell) with the substrate normal.<sup>2</sup> These films have been found to exhibit both the extraordinary Hall effect (EHE)<sup>2,3</sup> and the polar magneto-optic Kerr effect.<sup>4,5</sup> Refinements in the MBE growth technique<sup>6,7</sup> have led to progressively higher quality material. In this paper, we show that ultrathin epitaxial films of perpendicularly magnetized  $\tau(\text{Mn,Ni})\text{Al}$  grown on GaAs substrates yield remarkably ideal hyster-

etic extraordinary Hall characteristics. The high quality and uniformity of this material suggests that submicron binary storage elements, integrated with semiconductor access and control devices, could be fabricated.

## II. EXPERIMENTAL METHODS

Epitaxial (Mn,Ni)Al/AlAs/GaAs heterostructures were grown by a multistep MBE technique that has been described in previous references.<sup>2,6–8</sup>

The structural quality of the samples was characterized by x-ray scattering using Mo  $K_{\alpha 1}$  radiation from an 18-kW rotating anode generator and a triple-axis spectrometer with Ge(111) monochromator and analyzer crystals. Cross-sectional transmission electron microscopy (XTEM) using a JEOL 4000FX at 400 keV was performed to assess the sample morphology and to confirm and complement the x-ray findings.

The magnetic properties have been measured by vibrating sample magnetometry, magneto-optic Kerr effect and EHE. We discuss only the EHE results here, since these data are the most relevant for memory applications. The EHE characteristics were measured in multilayered photolithographically patterned Hall bars at room temperature. The measurement entails the recording of the transverse voltage generated while a dc current  $I_x$  is passed down the current axis of the Hall bar. The Hall voltage  $V_{xy}$  is measured as a function of applied magnetic field with the field  $H_z$  oriented parallel to the sample normal. The measured Hall voltage is proportional to the measurement current as given by the relation,  $V_{xy} = R_{xy}I_x$  where  $R_{xy}$  is the Hall “resistance.” This transverse resistance term can be expressed as  $\rho_{xy}/t$  where  $t$  is the film thickness and  $\rho_{xy}$  is the Hall resistivity. The saturation value of  $\rho_{xy}$  is a material property. Since the ordinary Hall effect (essentially the slope of the  $R_{xy}$  vs  $H_z$  plot at high fields when the measured area of the film becomes single domain) is negligible at these low fields compared to the EHE,  $\rho_x$  is taken to be the EHE resistivity. Note that the EHE is not due to the Lor-

<sup>a)</sup>Permanent address: Interuniversity Microelectronics Center (IMEC), Kapeldreef 75, B-3001 Leuven, Belgium.

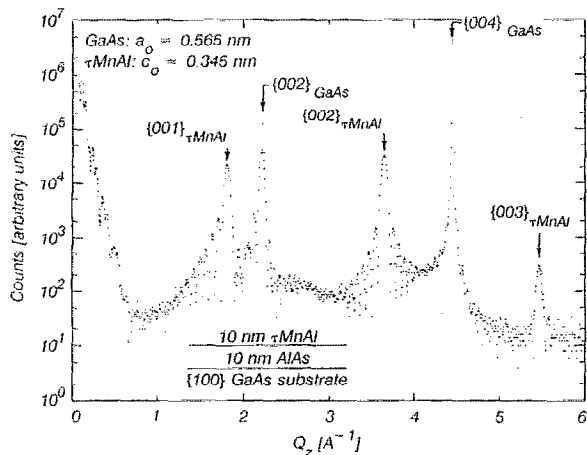


FIG. 1. X-ray Bragg reflectivity spectrum for momentum transfer normal to the substrate surface ( $Q_z$ ) from a 10-nm (nominal) thick film of  $\text{Mn}_{0.60}\text{Al}_{0.40}$  grown on a (001) GaAs substrate with a 10-nm AlAs intermediate buffer layer. Only the (001) peaks of the  $\tau$  MnAl phase are revealed, confirming the expected orientation relationship.

entz force; it is a measure of the  $z$  component of the net magnetization in the Hall cross and can thus be nonzero in zero applied field.

### III. RESULTS AND DISCUSSION

#### A. Structure and properties of coherent $\tau(\text{Mn,Ni})\text{Al}$ films

(Mn,Ni)Al films of 10-nm thickness with a range of compositions were characterized by the techniques described above. In this paper, we focus on the compositions  $\text{Mn}_{0.60-x}\text{Ni}_x\text{Al}_{0.40}$ ,  $x \leq 0.08$  for which nearly ideal structural and EHE characteristics were observed. Since samples in this range were found to be similar in structural quality and magnetic properties, we show data only from samples of one composition,  $\text{Mn}_{0.60}\text{Al}_{0.40}$ . Samples with compositions richer in Al generally exhibited poorer properties. A more comprehensive treatment of the broader composition range, including the effect of Ni substitution, will be published in Ref. 8.

Figure 1 shows the x-ray Bragg reflectivity from a  $\text{Mn}_{0.60}\text{Al}_{0.40}$  sample for crystallographic planes parallel to the (001) GaAs surface. The (002) and (004) peaks from the GaAs substrate and the 10-nm AlAs interface layer (the broader peaks at the base of the GaAs peaks), as well as the (001) peaks of  $\tau\text{Mn}_{0.60}\text{Al}_{0.40}$  are apparent, confirming that the (001) $\tau$ -phase planes of spacing 0.345 nm are parallel to the (001)GaAs surface. A scan through the (201) $\tau$  peak of the same sample in Fig. 2 shows that the *in-plane*  $Q_x$  component ( $Q_x = 2\pi/d_{100}$ ) of the (201) vector in momentum space is  $4.45 \text{ \AA}^{-1}$  corresponding to  $a_0 = 0.282 \text{ nm}$ , the value expected for *coherent* epitaxy of the  $\tau$  phase with  $\{200\}\tau \parallel \{400\}\text{GaAs}$ . If the  $\tau$ -phase film were relaxed to the expected bulk lattice parameters, the peak would be centered between 4.50 and  $4.54 \text{ \AA}^{-1}$  [note that the III-V substrate does not contribute significant intensity

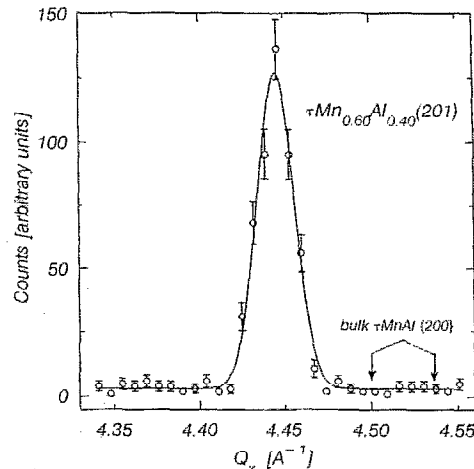


FIG. 2.  $Q_x$  component of (201)  $\tau\text{MnAl}$  peak as measured by x-ray scattering from the sample of Fig. 1.

to the (201) $\tau$  scan]. Coherent epitaxy was also observed for samples with 4 and 8 at. % Ni, as well as some samples with greater than 40 at. % Al (Ref. 8).

Observations of these films by XTEM were consistent with the x-ray results, showing clearly the (001) $\tau$  planes parallel to the GaAs substrate (Fig. 3 inset). The XTEM images also showed that the films were of uniform thickness and the interfaces were smooth and abrupt. Furthermore, a tweedlike strain contrast was visible in the coherent films, suggestive of the initial stages of decomposition into a two-phase mixture of the tetragonal  $\tau$  ( $c_0/a_0 = 1.28$ ) and cubic  $\kappa$  phases. These two phases have bulk in-plane lattice parameters that are 2% smaller and 5% larger than  $a_0/2$  (GaAs), respectively. Thus, it is plausible that the coherent MBE films with  $c_0/a_0$  values of about 1.22, between those of  $\kappa$  and bulk  $\tau$ , are composed of an intermediate thin-film phase that is stabilized by epitaxy.

The EHE characteristics of these films were found to be hysteretic with ideal switching characteristics; i.e., the films always switched completely within one increment of applied field (typically 100–200 Oe). Interpreted in terms of domain boundaries, this observation suggests that domain boundaries in the Hall cross (typically, an area of  $10 \times 10 \mu\text{m}$  or  $100 \times 100 \mu\text{m}$ ) were unstable, and were always swept across the region of the cross before a measurement could be made. For samples with 40 at. % Al, the



FIG. 3. XTEM image of a  $\tau\text{Mn}_{0.60}\text{Al}_{0.40}$  film. The inset is a higher magnification image revealing the (001) $\tau$  planes parallel to the substrate surface.

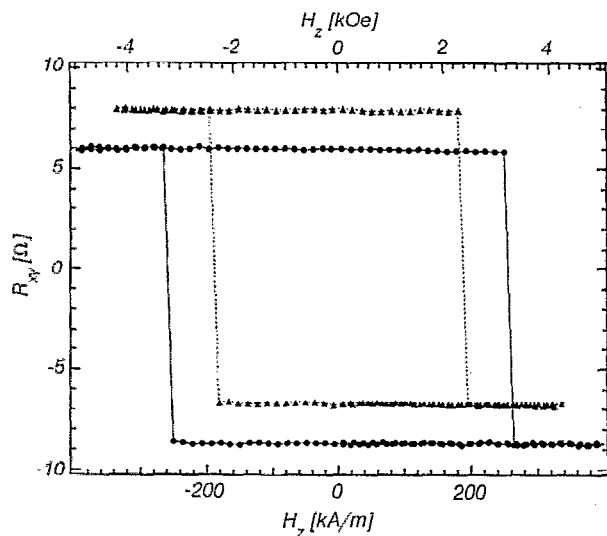


FIG. 4. EHE hysteresis loops from a patterned  $\text{Mn}_{0.60}\text{Al}_{0.40}$  section of the sample represented in Figs. 1–3. The measured region of the Hall bar was approximately  $10 \times 10 \mu\text{m}$ , the measurement current was  $1 \mu\text{A}$  and the data were recorded at room temperature. The two loops were recorded from the same Hall bar (and same set of contacts) but for different values of the maximum applied field (discussed in text). The loop with smaller coercive field is shifted up along the  $R_{xy}$  axis for clarity.

saturation value of  $\rho_{xy}$  was in the range of  $3.3\text{--}7.1 \mu\Omega\text{-cm}$  and coercive fields varied from  $1.6\text{--}3.4 \text{ kOe}$ .

In all samples with distinct switching characteristics, the coercive field was found to depend on the maximum value of the previously applied field of opposite polarity. For example, the EHE characteristics in Fig. 4 were recorded in measurements of the same Hall structure, but with differing maximum fields (the two characteristics are shifted vertically for clarity). This result suggests that higher applied fields drive domain walls to stronger pinning positions in the extremities of the patterned Hall structure (i.e., beyond the Hall cross). Thus the field required to switch is greater for larger previously applied maximum fields. The fact that strong pinning sites are not found within the Hall cross regions suggests that lithographically patterned features, rather than defects, may be the dominant pinning sites, a hypothesis that we have not yet tested experimentally.

## B. Device implications

In principle, binary information can be stored in these ultrathin films with magnetization “up” and “down” corresponding to “1” and “0.” The state of the film can be “read” by a measurement of the extraordinary Hall effect which yields, for a symmetric structure, a voltage whose polarity indicates the magnetic state of the film. Compared to the EHE resistivity of other materials [e.g.,  $3.3 \mu\Omega\text{-cm}$  for Gd-Co (Ref. 9) and  $1.1 \mu\Omega\text{-cm}$  for MnBi (Ref. 10)], the value of  $7 \mu\Omega\text{-cm}$  for  $\tau(\text{Mn,Ni})_{0.60}\text{Al}_{0.40}$  films is quite large, resulting in large voltage differences between the 0 and 1 states. For example, the voltage difference between

the two states would be  $14 \text{ mV}$  for a  $10\text{-nm}$ -thick film with  $\rho_{xy} = 7 \mu\Omega\text{-cm}$  and a measurement current  $I_x$  of  $1 \text{ mA}$ . For structures with small lateral dimensions, however, the maximum value of  $I_x$  will be limited by the maximum practical current density. Taking a value of  $10^6 \text{ A/cm}^2$  for the maximum current density during a short pulse, and assuming a Hall structure with  $1\text{-}\mu\text{m}$  width, the maximum current would be  $0.1 \text{ mA}$  and the voltage difference between the two states would be  $1.4 \text{ mV}$ .

Writing information is more problematic. Unlike the low-density magnetoresistive RAM which uses the small fields ( $\sim 10 \text{ Oe}$ ) generated by current lines carrying tens of mA to switch magnetic states, a high density magnetic RAM with submicron elements will require higher coercive fields to prevent crosstalk. Thus far, epitaxial  $\tau(\text{Mn,Ni})\text{Al}$  films with coercivities in the range of  $0.89\text{--}5 \text{ kOe}$  have been grown. The lowest coercivity was obtained with  $18 \text{ at.}\%$  Ni, yielding a structure with reduced tetragonality ( $c_0/a_0 = 1.09$ ) and magnetocrystalline anisotropy. Further reductions in coercivity may be possible in films with higher Ni content and lower tetragonality. Nevertheless, these relatively high coercivities would make switching with locally generated fields impractical. Thus, either Joule heating combined with local fields or more novel approaches, such as the current pulse mechanism for moving Bloch walls as described by Berger,<sup>11</sup> will be required.

## ACKNOWLEDGMENTS

The authors acknowledge S. J. Allen, Jr. and M. Leadbeater for their many contributions to the early stages of this work. Also, Rutherford backscattering data from B. J. Wilkens helped to calibrate film thicknesses and compositions. One of the authors (JDB) acknowledges NATO for financial assistance.

- <sup>1</sup> See recent review by E. D. Dahlberg, K. Riggs, and G. A. Prinz, *J. Appl. Phys.* **63**, 4270 (1988).
- <sup>2</sup> T. Sands, J. P. Harbison, M. L. Leadbeater, S. J. Allen, Jr., G. W. Hull, R. Ramesh, and V. G. Keramidas, *Appl. Phys. Lett.* **57**, 2609 (1990).
- <sup>3</sup> M. L. Leadbeater, S. J. Allen, Jr., F. DeRosa, J. P. Harbison, T. Sands, R. Ramesh, L. T. Florez, and V. G. Keramidas, *J. Appl. Phys.* **69**, 4689 (1991).
- <sup>4</sup> T. L. Cheeks, M. J. S. P. Brasil, T. Sands, J. P. Harbison, D. E. Aspnes, V. G. Keramidas, and S. J. Allen, Jr., *Appl. Phys. Lett.* **60**, 1393 (1992).
- <sup>5</sup> T. L. Cheeks, R. E. Nahory, T. Sands, J. P. Harbison, M. J. S. P. Brasil, H. L. Gilchrist, S. A. Schwarz, M. A. Pudensi, S. J. Allen, Jr., L. T. Florez, and V. G. Keramidas, *Inst. Phys. Conf. Ser. No. 120*, 101 (1992).
- <sup>6</sup> J. P. Harbison, T. Sands, R. Ramesh, L. T. Florez, B. J. Wilkens, and V. G. Keramidas, *J. Cryst. Growth* **111**, 978 (1991).
- <sup>7</sup> T. Sands, J. P. Harbison, S. J. Allen, Jr., M. L. Leadbeater, T. L. Cheeks, M. J. S. P. Brasil, C. C. Chang, R. Ramesh, L. T. Florez, F. DeRosa, and V. G. Keramidas, *Mater. Res. Soc. Symp. Proc.* **231**, 341 (1992).
- <sup>8</sup> J. P. Harbison, T. Sands, J. De Boeck, T. L. Cheeks, P. F. Miceli, M. Tanaka, L. T. Florez, B. J. Wilkens, H. L. Gilchrist, and V. G. Keramidas, paper presented at the MBE VII 1992 Conference in Schwabisch Gmund, Germany, August 24–28, 1992, to be published in *J. Cryst. Growth*.
- <sup>9</sup> K. Okamoto, T. Shirakawa, S. Matsushita, and V. Sakurai, *IEEE Trans. Magn.* **MAG-10** (3), 799 (1974).
- <sup>10</sup> K. Okamoto, M. Tanaka, S. Matsushita, and Y. Sakurai, *AIP Conf. Proc. No. 34*, 55 (1976).
- <sup>11</sup> See L. Berger, *J. Appl. Phys.* **71**, 2721 (1992), and references therein.